Real-time three-dimensional optical coherence tomography image-guided core-needle biopsy system

Wei-Cheng Kuo,[1,2,3] Jongsik Kim,[1] Nathan D. Shemonski,[1,2] Eric J. Chaney,[1] Darold R. Spillman, Jr.,[1] and Stephen A. Boppart[1,2,4,*]

[1]*Beckman Institute for Advanced Science and Technology, University of Illinois at Urbana-Champaign, Urbana, IL 61801, USA*
[2]*Department of Electrical and Computer Engineering, University of Illinois at Urbana-Champaign, Urbana, IL 61801, USA*
[3]*Department of Electrical Engineering, National Taiwan University, 106 Taiwan*
[4]*Departments of Bioengineering and Internal Medicine, University of Illinois at Urbana-Champaign, Urbana, IL 61801, USA*
*boppart@illinois.edu

Abstract: Advances in optical imaging modalities, such as optical coherence tomography (OCT), enable us to observe tissue microstructure at high resolution and in real time. Currently, core-needle biopsies are guided by external imaging modalities such as ultrasound imaging and x-ray computed tomography (CT) for breast and lung masses, respectively. These image-guided procedures are frequently limited by spatial resolution when using ultrasound imaging, or by temporal resolution (rapid real-time feedback capabilities) when using x-ray CT. One feasible approach is to perform OCT within small gauge needles to optically image tissue microstructure. However, to date, no system or core-needle device has been developed that incorporates both three-dimensional OCT imaging and tissue biopsy within the same needle for true OCT-guided core-needle biopsy. We have developed and demonstrate an integrated core-needle biopsy system that utilizes catheter-based 3-D OCT for real-time image-guidance for target tissue localization, imaging of tissue immediately prior to physical biopsy, and subsequent OCT imaging of the biopsied specimen for immediate assessment at the point-of-care. OCT images of biopsied *ex vivo* tumor specimens acquired during core-needle placement are correlated with corresponding histology, and computational visualization of arbitrary planes within the 3-D OCT volumes enables feedback on specimen tissue type and biopsy quality. These results demonstrate the potential for using real-time 3-D OCT for needle biopsy guidance by imaging within the needle and tissue during biopsy procedures.

OCIS codes: (170.4500) Optical coherence tomography; (120.3890) Medical optics instrumentation; (110.6880) Three-dimensional image acquisition; (170.1610) Clinical applications.

References and Links

1. M. Kriege, C. T. Brekelmans, C. Boetes, P. E. Besnard, H. M. Zonderland, I. M. Obdeijn, R. A. Manoliu, T. Kok, H. Peterse, M. M. Tilanus-Linthorst, S. H. Muller, S. Meijer, J. C. Oosterwijk, L. V. Beex, R. A. Tollenaar, H. J. de Koning, E. J. Rutgers, and J. G. Klijn; Magnetic Resonance Imaging Screening Study Group, "Efficacy of MRI and mammography for breast-cancer screening in women with a familial or genetic predisposition," N. Engl. J. Med. **351**(5), 427–437 (2004).
2. D. A. Bluemke, C. A. Gatsonis, M. H. Chen, G. A. DeAngelis, N. DeBruhl, S. Harms, S. H. Heywang-Köbrunner, N. Hylton, C. K. Kuhl, C. Lehman, E. D. Pisano, P. Causer, S. J. Schnitt, S. F. Smazal, C. B. Stelling,

P. T. Weatherall, and M. D. Schnall, "Magnetic resonance imaging of the breast prior to biopsy," JAMA **292**(22), 2735–2742 (2004).

3. C. Wiratkapun, B. Wibulpholprasert, S. Wongwaisayawan, and K. Pulpinyo, "Nondiagnostic core needle biopsy of the breast under imaging guidance: result of rebiopsy," J. Med. Assoc. Thai. **88**(3), 350–357 (2005).

4. R. M. Pijnappel, M. van den Donk, R. Holland, W. P. Mali, J. L. Peterse, J. H. Hendriks, and P. H. Peeters, "Diagnostic accuracy for different strategies of image-guided breast intervention in cases of nonpalpable breast lesions," Br. J. Cancer **90**(3), 595–600 (2004).

5. P. M. Rich, M. J. Michell, S. Humphreys, G. P. Howes, and H. B. Nunnerley, "Stereotactic 14G core biopsy of non-palpable breast cancer: what is the relationship between the number of core samples taken and the sensitivity for detection of malignancy?" Clin. Radiol. **54**(6), 384–389 (1999).

6. D. D. Dershaw, E. A. Morris, L. Liberman, and A. F. Abramson, "Nondiagnostic stereotaxic core breast biopsy: results of rebiopsy," Radiology **198**(2), 323–325 (1996).

7. D. Huang, E. A. Swanson, C. P. Lin, J. S. Schuman, W. G. Stinson, W. Chang, M. R. Hee, T. Flotte, K. Gregory, C. A. Puliafito, and J. G. Fujimoto, "Optical coherence tomography," Science **254**(5035), 1178–1181 (1991).

8. B. E. Bouma and G. J. Tearney, *Handbook of Optical Coherence Tomography* (Informa Healthcare, London, 2001).

9. A. M. Zysk, F. T. Nguyen, A. L. Oldenburg, D. L. Marks, and S. A. Boppart, "Optical coherence tomography: a review of clinical development from bench to bedside," J. Biomed. Opt. **12**(5), 051403 (2007).

10. F. T. Nguyen, A. M. Zysk, E. J. Chaney, J. G. Kotynek, U. J. Oliphant, F. J. Bellafiore, K. M. Rowland, P. A. Johnson, and S. A. Boppart, "Intraoperative evaluation of breast tumor margins with optical coherence tomography," Cancer Res. **69**(22), 8790–8796 (2009).

11. K. Bizheva, A. Unterhuber, B. Hermann, B. Povazay, H. Sattmann, A. F. Fercher, W. Drexler, M. Preusser, H. Budka, A. Stingl, and T. Le, "Imaging *ex vivo* healthy and pathological human brain tissue with ultra-high-resolution optical coherence tomography," J. Biomed. Opt. **10**(1), 011006 (2005).

12. W. Wieser, B. R. Biedermann, T. Klein, C. M. Eigenwillig, and R. Huber, "Multi-megahertz OCT: High quality 3D imaging at 20 million A-scans and 4.5 GVoxels per second," Opt. Express **18**(14), 14685–14704 (2010).

13. A. M. Zysk and S. A. Boppart, "Computational methods for analysis of human breast tumor tissue in optical coherence tomography images," J. Biomed. Opt. **11**(5), 054015 (2006).

14. M. Mujat, R. D. Ferguson, D. X. Hammer, C. Gittins, and N. Iftimia, "Automated algorithm for breast tissue differentiation in optical coherence tomography," J. Biomed. Opt. **14**(3), 034040 (2009).

15. A. M. Zysk, F. T. Nguyen, E. J. Chaney, J. G. Kotynek, U. J. Oliphant, F. J. Bellafiore, P. A. Johnson, K. M. Rowland, and S. A. Boppart, "Clinical feasibility of microscopically-guided breast needle biopsy using a fiber-optic probe with computer-aided detection," Technol. Cancer Res. Treat. **8**(5), 315–321 (2009).

16. G. J. Tearney, M. E. Brezinski, B. E. Bouma, S. A. Boppart, C. Pitris, J. F. Southern, and J. G. Fujimoto, "*In vivo* endoscopic optical biopsy with optical coherence tomography," Science **276**(5321), 2037–2039 (1997).

17. L. Huo, J. Xi, Y. Wu, and X. Li, "Forward-viewing resonant fiber-optic scanning endoscope of appropriate scanning speed for 3D OCT imaging," Opt. Express **18**(14), 14375–14384 (2010).

18. X. Li, C. Chudoba, T. Ko, C. Pitris, and J. G. Fujimoto, "Imaging needle for optical coherence tomography," Opt. Lett. **25**(20), 1520–1522 (2000).

19. A. M. Zysk, S. G. Adie, J. J. Armstrong, M. S. Leigh, A. Paduch, D. D. Sampson, F. T. Nguyen, and S. A. Boppart, "Needle-based refractive index measurement using low-coherence interferometry," Opt. Lett. **32**(4), 385–387 (2007).

20. N. V. Iftimia, M. Mujat, T. Ustun, R. D. Ferguson, V. Danthu, and D. X. Hammer, "Spectral-domain low coherence interferometry/optical coherence tomography system for fine needle breast biopsy guidance," Rev. Sci. Instrum. **80**(2), 024302 (2009).

21. A. M. Zysk, D. L. Marks, D. Y. Liu, and S. A. Boppart, "Needle-based reflection refractometry of scattering samples using coherence-gated detection," Opt. Express **15**(8), 4787–4794 (2007).

22. W. Jung, W. Benalcazar, A. Ahmad, U. Sharma, H. Tu, and S. A. Boppart, "Numerical analysis of gradient index lens-based optical coherence tomography imaging probes," J. Biomed. Opt. **15**(6), 066027 (2010).

23. J. H. Hwang, M. J. Cobb, M. B. Kimmey, and X. Li, "Optical coherence tomography imaging of the pancreas: a needle-based approach," Clin. Gastroenterol. Hepatol. **3**(7 Suppl 1), S49–S52 (2005).

24. B. C. Quirk, R. A. McLaughlin, A. Curatolo, R. W. Kirk, P. B. Noble, and D. D. Sampson, "*In situ* imaging of lung alveoli with an optical coherence tomography needle probe," J. Biomed. Opt. **16**(3), 036009 (2011).

25. D. Lorenser, X. Yang, R. W. Kirk, B. C. Quirk, R. A. McLaughlin, and D. D. Sampson, "Ultrathin side-viewing needle probe for optical coherence tomography," Opt. Lett. **36**(19), 3894–3896 (2011).

26. K. Zhang and J. U. Kang, "Real-time 4D signal processing and visualization using graphics processing unit on a regular nonlinear-k Fourier-domain OCT system," Opt. Express **18**(11), 11772–11784 (2010).

27. J. Rasakanthan, K. Sugden, and P. H. Tomlins, "Processing and rendering of Fourier domain optical coherence tomography images at a line rate over 524 kHz using a graphics processing unit," J. Biomed. Opt. **16**(2), 020505 (2011).

1. Introduction

Cell or tissue specimens are needed for the pathological diagnosis of disease. Clinical imaging modalities such as magnetic resonance imaging (MRI), computed tomography (CT),

ultrasound imaging, and planar x-ray are standard non-invasive technologies used for screening or identifying abnormal masses. Obtaining cell or tissue specimens for pathological diagnosis, however, often requires fine-needle or core-needle biopsy procedures, respectively, to extract specimens from patients. For example, fine-needle biopsies are performed on thyroid masses detected on physical examination or ultrasound imaging, and collections of needle-aspirated cells are viewed by cytopathologists. Core-needle biopsies (CNBs), which extract larger tissue cores to maintain tissue architecture, are frequently guided by ultrasound imaging, stereotactic x-ray imaging, or MRI and used in evaluating breast masses found on x-ray or MR mammography. Lung nodules found on planar chest x-ray images are often biopsied with core-needles under x-ray CT guidance.

Many studies have shown that MRI significantly improves the screening in women susceptible to breast cancer, and the use of MRI in breast imaging is rapidly expanding. This success can be attributed to the capability of MRI to resolve and identify small lesions or micro-calcifications. The sensitivity of MRI (71.1%) was found to be much higher than that of x-ray mammography (40%) [1]. In this study, MRI detected 20 cancers that were missed by x-ray mammography or clinical breast examination among 45 cancers in total. More than half of these invasive tumors were smaller than 10 mm [1]. Despite its high sensitivity, the specificity of MRI screening is not satisfactory, generally around 68% [2]. Early detection of suspicious lesions by MRI or other non-invasive imaging techniques has placed an increased demand on accurately localizing biopsy needles to these small lesions, particularly for percutaneous CNB procedures [3].

The current diagnostic efficacy of CNB is therefore problematic. In addition to high rates of underestimating high-risk and ductal carcinoma [4], large core-needle biopsy (LCNB) shows a relatively high miss rate. The miss rates for various diagnostic strategies differ, but include: 2% for needle-localized breast open biopsy (NLBB), 12% for LCNB, 3% for LCNB in a study setting, and 5% for fine needle aspiration [4]. For an 18-gauge needle with 2 or 3 passes, stereotactic-guided LCNB has a disappointing 66.6% miss rate [4]. Today, physicians often take 6 or more cores in one lesion in an effort to reduce this miss rate and obtain a sufficient amount of tissue for diagnosis [4,5]. Similar results were presented by another study in which 16% of the subjects underwent repeat biopsy procedures, and among them, 39% had malignancies [6]. The sensitivity of CNB depends considerably on the properties of the lesions, the experience of the physicians and technicians, and the performance characteristics of the biopsy machines [3,4]. Regardless, there is a strong need to improve the technology and methodology to more accurately identify and localize increasingly smaller lesions, to provide real-time image-guidance within the needle itself and during the biopsy, and to image the biopsied specimens with high-resolution at the point-of-care so that the physician can determine if the target abnormal lesion has been appropriately biopsied prior to ending the procedures and sending the tissue specimens for sectioning, staining, and histopathological analysis.

Optical coherence tomography (OCT) has emerged as a fast high-resolution 3-D biomedical imaging modality that can be used to identify pathological tissues including many types of cancers in the breast, lung, thyroid, kidney, liver, and brain, among many others [7–11]. With axial-scan line rates of tens to hundreds of thousands of Hertz, imaging resolution of 2-10 microns, and imaging depth of 1-2 mm in highly scattering media, OCT is a suitable candidate for real-time 3-D assessment of biological tissue [12]. Moreover, computational algorithms are being developed to rapidly perform computer-aided detection, such as in breast tissue [13–15]. The miniaturization of OCT beam-delivery optics to a few hundreds of microns [16,17] permits integration of sample-arm fibers and micro-optics within fine- and core-needle biopsy needles to provide minimally-invasive imaging within soft tissues or suspicious lesions. Numerous groups have demonstrated the use of optical needles for OCT imaging and diagnostics [18–25]. However, these optical needles typically consist of a single optical fiber and micro-optics within a single metal needle barrel, and require that the OCT

needle be removed from the tissue prior to inserting a second needle-biopsy device to physically biopsy tissue and retrieve tissue specimens. To date, there has been no demonstration of an OCT-guided needle-biopsy device or system that permits physical tissue biopsy immediately after OCT guided placement and lesion localization, and no optical needle system has been demonstrated that enables 3-D OCT imaging of the physically biopsied specimen to assess the quality of the biopsied specimen prior to sending to the pathology department for histopathological processing and evaluation.

In this paper, we introduce the design, development, and demonstration of a 3-D OCT-guided core-needle biopsy system that permits the real-time OCT-guided positioning of the biopsy needle, 3-D OCT of tissue regions immediately prior to tissue biopsy, and subsequent 3-D OCT of the biopsied specimen to visualize and confirm if abnormal lesion tissue was adequately sampled prior to histopathological analysis. Our integrated system design includes a re-designed and engineered hand-held core-needle biopsy device that leverages the advanced development of both a commercial vacuum-assisted core-needle breast biopsy system (Hologic, Inc.) and a commercial catheter-based 3-D OCT system (St. Jude Medical, Inc.) to permit real-time OCT guidance during use. We believe this system and methodology offers the best opportunity to reduce non-diagnostic sampling rates for small non-palpable lesions, to reduce the number of tissue biopsy cores necessary to adequately sample the lesion and surrounding tissue, and to potentially alleviate differences in non-diagnostic sampling rates between experienced and inexperienced physicians due to the fact that with this method, we are able to accurately select regions of interest while the needle is still in the tissue.

2. Materials and methods

The integrated system developed for these studies consisted of three components: 1) a modified core-needle biopsy hand-piece, 2) a vacuum-assisted breast needle biopsy console (Suros, model ATEC Pearl Breast Biopsy System, Hologic, Inc.), and 3) a catheter-based OCT system (Model C7XR, St. Jude Medical, Inc.) (Fig. 1).
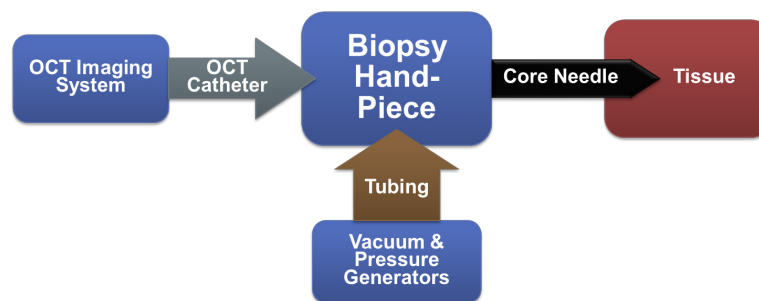

Fig. 1. Overview of the 3-D OCT-guided vacuum-assisted core-needle breast biopsy system.

This integrated system was designed to leverage the advantages of commercial systems, yet develop a new design and concept for a core-needle biopsy hand-piece that can be optically-guided in real-time by OCT. For guidance during needle insertion, positioning, and biopsy, and to acquire a 3-D OCT image of the biopsied specimen to provide a microscopic "first look" of the specimen prior to sending for histopathological sectioning and analysis, the OCT catheter is inserted into the needle-biopsy hand-piece which has been modified to include optical windows at specific locations. The design and methodology presented here maintains the full functionality of the vacuum-assisted core-needle breast biopsy system as well as the catheter-based OCT system.

2.1. OCT-guided vacuum-assisted core-needle biopsy hand-piece

The standard vacuum-assisted core-needle biopsy hand-piece mechanically operates via pneumatic pressure and vacuum (Fig. 2). When attached to the system console and armed, a

pneumatic motor drives a cutting cannula forward to cover the biopsy channel and produce a smooth outer needle barrel prior to insertion into tissue. When the needle tip has been positioned at the tissue site for biopsy (typically guided under external imaging by stereotactic x-ray or ultrasound imaging), a foot pedal switch initiates a vacuum to draw the cutting cannula back, thereby exposing the biopsy channel, and allowing a small region of tissue to be drawn under vacuum into the biopsy channel region. We modified the biopsy extraction sequence by putting a manual break between the opening of the cutting cannula with the applied vacuum, and the closing of cutting cannula. Following another activation switch, the outer cutting cannula closes with a rotating/spinning motion and shears off the tissue specimen. We also included a second manual break in the process, before the tissue is subsequently drawn back into a tissue collection trap by the applied vacuum where it can be later retrieved and placed in formalin for histopathological processing.
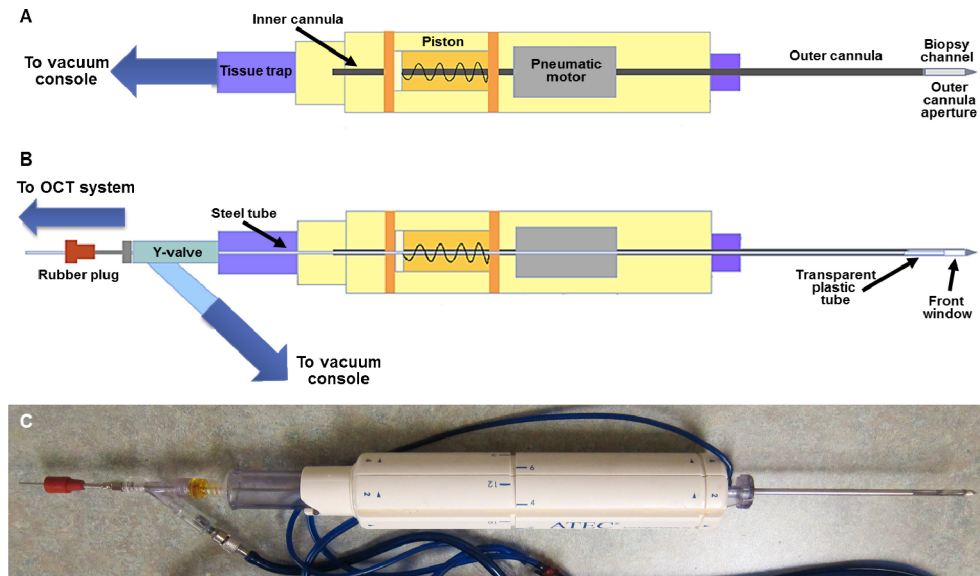

Fig. 2. Schematics and photograph of the modified vacuum-assisted core-needle biopsy hand-piece for 3-D OCT-guided procedures. (A) Schematic of original hand-piece components. Using pressure and vacuum, the unit mechanically opens and closes a cutting cannula, and vacuum is used to both draw tissue into the biopsy channel prior to biopsy, and to draw biopsied tissue back into a tissue trap for retrieval. (B) Schematic of modified hand-piece, which includes the addition of a transparent front window for real-time OCT guidance, the addition of a long steel/plastic tube through which the OCT catheter is inserted, and a Y-valve to allow both linear access for the OCT catheter and the vacuum/pressure tube connection. (C) Photograph of modified hand-piece.

Numerous essential modifications were made to the biopsy hand-piece (ATEC 0912-20, 9 Gauge) to enable real-time 3-D OCT guidance (Fig. 2). First, an optical window was added at the distal tip of the 12 cm-long 9 Gauge core-biopsy needle by removing a portion of the metal needle barrel to lengthen the tissue biopsy channel by 7.6 mm. In addition, the cutting cannula was also shortened by 8.6 mm to preserve the cutting/biopsy function of the device, while providing an optical window for OCT imaging. A transparent hemi-cylindrical Pyrex glass segment was used in place of the removed metal barrel segment. Second, a 50 cm-long metal tube (1.6 mm outer diameter) with a transparent plastic tube (1.5 mm outer diameter) attached to the distal end was fabricated and inserted into the hand-piece, running the entire length up to the front window region, and located within the metal needle barrel. Given the 1.5 mm outer diameter of the plastic tube, and the 3.0 mm inner diameter of the metal needle barrel, the added plastic tube filled 25% of the cross-sectional area of the needle barrel, resulting in a similar reduction in the cross-sectional area available for the biopsied tissue

specimen. Fortuitously, many core-needle biopsy hand-pieces used for tissue biopsy have a large-bore hollow central tube through which biopsied tissue is drawn via vacuum into a proximal tissue collection chamber or trap. This hollow central tube provided ready access for an OCT catheter (Fig. 3). The distal transparent plastic tube was positioned to span the tissue biopsy channel and extend up to where the front window was located. This tube enabled 3-D OCT imaging of the tissue (in a cylindrical wedge-shaped volume) during needle positioning, and both immediately prior to biopsy and following biopsy when the cutting cannula had closed and while the biopsied tissue specimen remained in the biopsy channel. Third, the
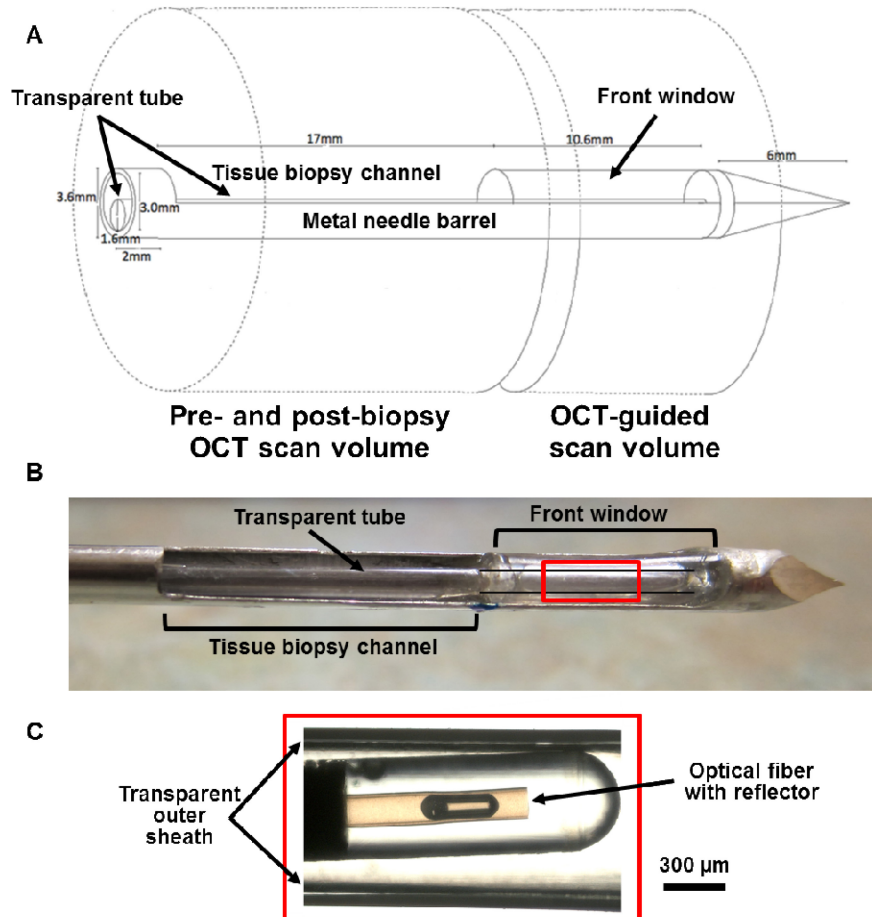

Fig. 3. Modified hand-piece tip detail. (A) Schematic of the modifications made to the core-needle tip including lengthening of the biopsy channel to accommodate a front window, and the addition of a transparent tube (attached to the distal end of the added metal tube) through which the OCT catheter is passed for imaging. (B) Photograph of modified tip with the cutting cannula retracted to expose the tissue biopsy channel. The plastic tube can be observed in the tissue biopsy channel, with its end opening into the front window region (parallel black lines and red box are added to highlight the OCT catheter tip location when fully inserted into the needle). (C) High-magnification photograph of the distal end of the OCT catheter. This catheter, with its own transparent outer sheath, is positioned either in the front window region or within the tissue biopsy channel for imaging. The scale bar refers only to the photograph in (C). The possible OCT scan volumes during needle tip guidance and during pre- and post-biopsy are shown in (A). Only a cylindrical wedge of 3-D OCT data is possible due to a portion of the radial image being obscured by the metal needle barrel. However, additional 3-D OCT data from other wedge sections can be obtained by rotating the needle about its long axis.

proximal end of the hand-piece, where the tissue trap was located, was modified with the addition of a Y-connector to allow for the straight passage of the long metal tube and insertion place for the OCT catheter. The modified tissue trap was sealed, and epoxy glue was also applied immediately proximal to the front window to hold a vacuum. The vacuum hose from the biopsy system console was attached to the other port of the Y-connector (Fig. 2).

'2.2. OCT-guided vacuum-assisted core-needle biopsy procedure

The expected operation and use of this 3-D OCT image-guided needle biopsy system is summarized. Before inserting the needle into tissue, the system is initiated by closing the front aperture over the tissue biopsy chamber and starting the vacuum in the inner bore of the cannula, preparing the system for biopsy mode. It is important that the aperture of this biopsy chamber be closed prior to insertion and advancement into tissue to minimize tissue injury. The OCT catheter (Dragonfly model C7, St. Jude Medical, Inc.) is then inserted into the proximal end of the hand-piece via the small metal/plastic tube. The OCT catheter is first advanced within the hand-piece all the way until the catheter tip reaches the tip of the needle, making OCT imaging possible through the transparent front window. Under real-time OCT guidance (typically with high-speed rotational imaging at one fixed position without automated pull-back), the needle is inserted into tissue toward its target, relying on the radial OCT image data to provide immediate feedback and to differentiate normal from abnormal regions of tissue.

Once the needle tip has been guided to and is located within the target tissue site, the needle is then advanced forward by ~1 cm to bring the target tissue into position over the tissue biopsy channel. The OCT catheter can then either be retracted by ~1 cm to position the imaging volume within the transparent tube segment located along the bottom of the tissue biopsy channel, or under system control, the catheter fiber/micro-optics can be pulled back within the stationary catheter sheath so that the 3-D OCT data collection occurs in the region of the biopsy channel. Next, following foot pedal activation, the inner cannula retracts, exposing the tissue biopsy channel and allowing the vacuum to draw the adjacent tissue of interest into the chamber prior to biopsy. The vacuum also serves to draw the tissue of interest in and around the plastic tube containing the OCT catheter, bringing the tissue within the optical depth-of-field of the catheter. At this time, 3-D OCT volumes with automated pull-back can be collected to confirm the target tissue first visualized through the front window during needle placement. The needle can also be rotated or re-positioned (with or without vacuum) over small distances with the biopsy channel open and during OCT imaging to further validate the tissue site prior to physical biopsy. Once confirmed and following activation, the cutting cannula advances forward at high speed in a helical spinning pattern to cut the tissue located within the chamber. After the cutting cannula has closed the biopsy channel and has retained the biopsy specimen, additional 3-D OCT of the biopsied tissue can be performed to assess the specimen at the point-of-care, and prior to being sent to pathology for histological processing. The biopsied tissue specimen remains in the biopsy chamber until the vacuum generated by the console draws the tissue specimen through the hand-piece toward the proximal end where it comes to rest in the tissue trap and is later removed, placed in a fixative, and sent for histopathological processing and analysis.

2.3. OCT system and imaging parameters

The commercial OCT catheter (C7 Dragonfly Intravascular Imaging Catheter, St. Jude Medical, Inc.) used in this study was 1.35 m long, had an outer diameter of 0.9 mm, a 4.83 mm imaging depth range, and specified axial and transverse resolutions of 20 µm and 25-60 µm, respectively. Imaging was performed at an axial scan rate of 50 kHz, with either stationary (no pull-back) radial imaging up to 100 frames per second, or variable pull-back distances of 0-54 mm over 0-5 s. When performing stationary radial imaging, the system acquired 4032 radial A-scans per radial image. However, when performing radial imaging

during pull-back (25 mm pull-back, 1000 images, ~25 µm spacing between images), only 504 radial A-scans per radial image were acquired, resulting in under-sampling of the tissue microstructure. Two-dimensional radial OCT images or 3-D cylindrical OCT volumes of data were exported from the system in tiff format, and additional 3-D volume rendering, visualization, and computational sectioning at *en face* and cross-sectional planes was done using commercial software (Amira, Inc.).

To determine the effects of the front window and transparent plastic tube on the OCT imaging resolution, a 3-D tissue phantom was constructed using sub-resolution (<5 µm) point-scatterers of TiO_2 suspended in a polydimethylsiloxane (PDMS) medium (5 µg of TiO_2 and 7 g of PDMS). The 3-D tissue phantom was placed over the front window and open biopsy channel of the core-needle biopsy probe containing the OCT catheter, and OCT images were collected through the front window (operating in stationary radial imaging mode) as well as through the plastic tubing (operating in pull-back radial imaging mode). Measurements were made from the images of point-scatterers to determine the 3-D PSFs, corresponding to the axial and lateral resolutions (FWHM). The axial resolution of the beam passing through either the front window or the plastic tubing was measured to be 19 µm, which is consistent with the axial resolution from the catheter alone (20 µm). The lateral resolution of the beam passing through the front window was measured to be 24-26 µm, with no obvious asymmetry due to astigmatism from the curved glass window. The lateral resolution of the beam passing through the plastic tubing in the biopsy channel was measured to be 16-24 µm, however more accurate measurements were limited by the under-sampling of the image data during the automated pull-back sequence. These measured transverse resolution values are all consistent with those from the catheter alone (25-60 µm), with no obvious effects from astigmatism from the plastic tubing.

2.4. Tissue specimens and histological processing

To replicate the presence of abnormal tumor tissue within a larger mass of normal tissue, a ~0.5 cm mass of lymphoid tissue with histologically-proven lymphoma from the thoracic cavity of a cat was wrapped with normal chicken breast tissue and inserted into a 50 ml, conical tube. These tissue types were chosen to present a relatively challenging case for detecting subtle differences between two highly-scattering, relatively homogeneous-appearing tissue types under OCT. In addition, the needle-biopsy of lymph nodes and lymphoid tissue is a common medical procedure in the evaluation of potentially metastatic cancer. The needle was subsequently inserted into the tissue contained within the conical tube and under real-time OCT, guided to the tumor tissue site for physical biopsy. Multiple biopsy specimens were acquired, fixed in formalin, and processed, sectioned, and stained with hematoxylin and eosin for histological examination. Biopsy specimens were computationally sectioned both in cross-section (corresponding to the orientation of radial OCT images) and in longitudinal orientation (corresponding to longitudinal B-mode OCT images) for co-registration and comparison with the acquired OCT images.

3. Results

3.1. Guiding window and real-time cross-sectional imaging

Insertion and needle-tip placement was performed under real-time cross-sectional radial OCT imaging with the OCT catheter tip advanced all the way to the inner tip of the needle, where the OCT beam could pass out through the front window (Fig. 3). Representative image data and corresponding cross-sectional histology are shown in Fig. 4, along with a video (Media 1).

Figure 4(A) shows one radial OCT image that reveals the inner OCT catheter and its protective sheath, the transparent front window and the tissue located outside, and the highly scattering metal needle barrel. Note that at this front-window location, approximately 180°
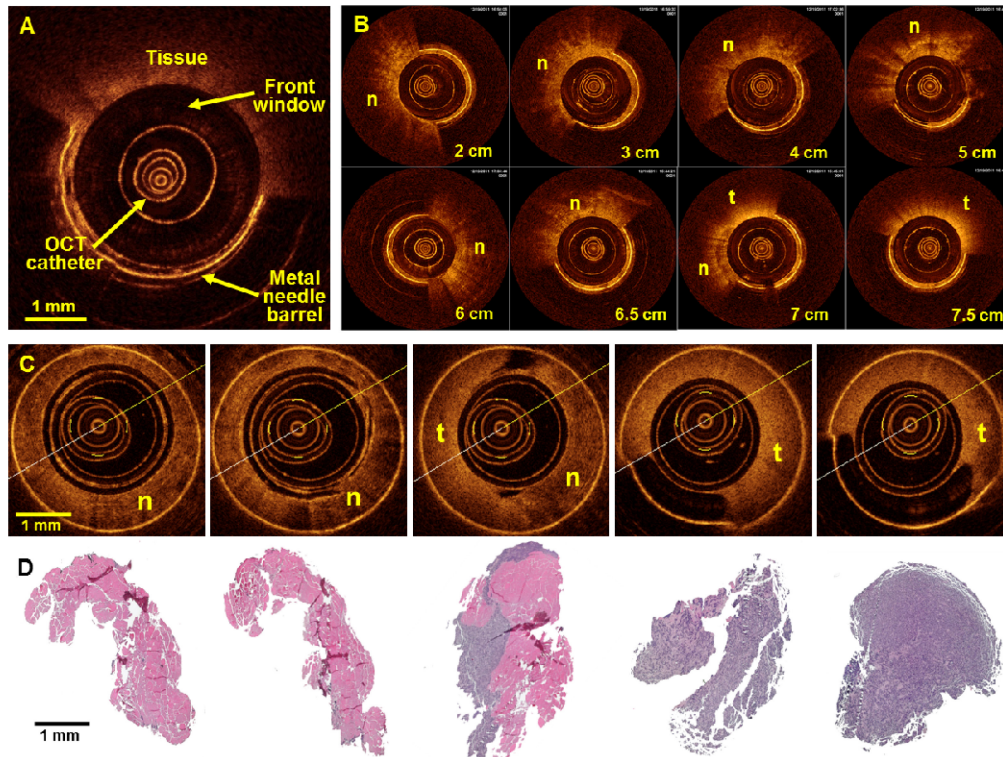
Fig. 4. Real-time cross-sectional radial OCT-guided needle placement and biopsy. (A) Radial OCT image acquired by imaging through the transparent front window. Interfaces of the OCT catheter sheath, tissue, and metal needle barrel are evident. (B) Series of radial OCT images collected in real-time as the needle was advanced into tissue. Distance values are relative to the tissue surface. (C) Series of radial OCT images from a 3-D volume collected from a biopsied tissue specimen retained within the closed biopsy channel (as evident by the outer full-circumference highly-scattering metal needle barrel). (D) Cross-sectional histology corresponding to the locations imaged in (C). The lymphoid tumor tissue is staining darker purple while the normal tissue is lighter pink. Included video (Media 1) of (B) was collected near the interface between the normal and tumor tissue.

of the OCT radial scan is usable for tissue imaging with the other 180° obscured by the metal needle barrel.

Figure 4(B) shows a sequence of 2-D radial OCT images at different positions as the needle was inserted into the tissue. Normal tissue is evident at the 2–6.5 cm positions. The denser more homogeneous lymphoid tumor tissue becomes apparent at the 7 cm position. From this series, needle barrel rotation is also observed as the needle was inserted into the tissue. Figure 4(C) shows a series of 2-D radial OCT images from a 3-D OCT volume of a tissue specimen after it has been physically biopsied and is being retained within the closed biopsy channel. Regions of normal and tumor tissue are observed. Note that the last two images in Fig. 4(C) show dark low-scattering regions corresponding to where there was an air space between the transparent tube and the inner wall of the needle barrel, while the other images show that the transparent tube had lifted away from the metal needle barrel, with tissue encircling the transparent tube while under vacuum. Corresponding cross-sectional histology sections are shown in Fig. 4(D), with each sectioned at the approximate location of the images shown in Fig. 4(C).

3.2. Three-dimensional OCT and visualization of pre- and post-biopsy tissue

The needle geometry permits 3-D OCT data collection within the biopsy channel both before and after the physical biopsy has been taken. Imaging immediately prior to physical biopsy enables more precise positioning of the needle to biopsy the tissue of interest. The 3-D OCT data set is a cylindrical volume composed of both a cylindrical wedge of tissue data and the remaining data from the metal needle barrel. Computational sectioning of the 3-D data set permits visualization of the tissue in multiple ways. Figures 5 and 6 show longitudinal (along the long axis of the needle) *en face* and cross-sectional images extracted from the 3-D OCT data set, illustrating the multiple planes that can be extracted to visualize the tissue structure either before or immediately after the physical tissue biopsy.

In this current design, the tissue drawn into the biopsy channel and around the OCT catheter is within the optical depth-of-field of the catheter. The transparent walls of the catheter sheath and plastic tube can be visualized in the 3-D reconstructions (Figs. 5(A) and 6(A)), as well as the tissue located around the plastic tube. The images collected of the tissue show variations in scattering structures, with the lymphoid tumor tissue exhibiting a more homogeneous scattering pattern within the OCT images (Figs. 4(B,C) and 5(B,C)). The tissue regions imaged in Figs. 6(B) and 6(C), show more subtle variations in scattering due to the differences in cellular organization and tissue structure in the tumor regions versus areas of necrotic tissue, verified by the corresponding histology. The longitudinal images shown in Figs. 5 and 6 also exhibit lower lateral resolution and contrast due to the inherent under-sampling of the automated pull-back imaging sequence, as described in the Materials and Methods.
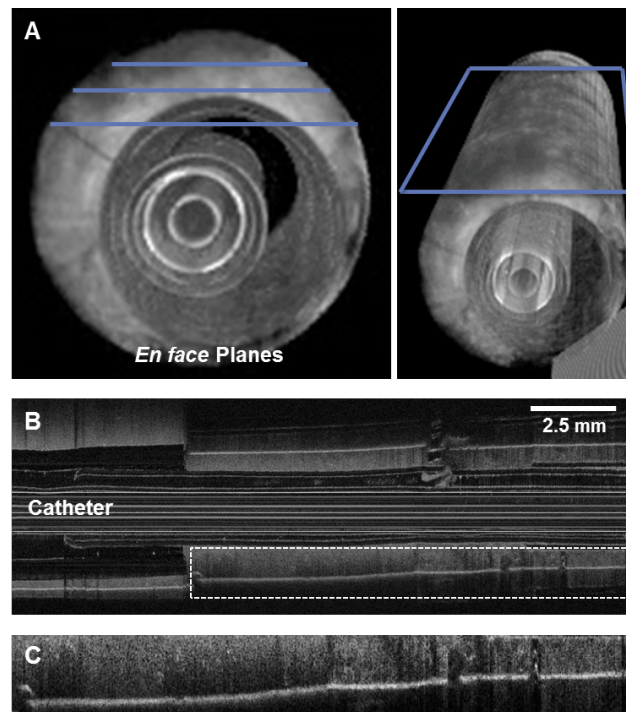

Fig. 5. Visualization of longitudinal (long-axis) *en face* planes of tissue data prior to tissue biopsy. (A) Three-dimensional renderings of the acquired OCT data set, illustrating orientation of *en face* planes relative to catheter and needle. (B) *En face* plane extracted at a plane that includes not only the tissue but also the transparent plastic tube and sheath housing the OCT catheter. (C) Enlarged region of imaged tissue, from the region indicated by the white dashed box in (B).
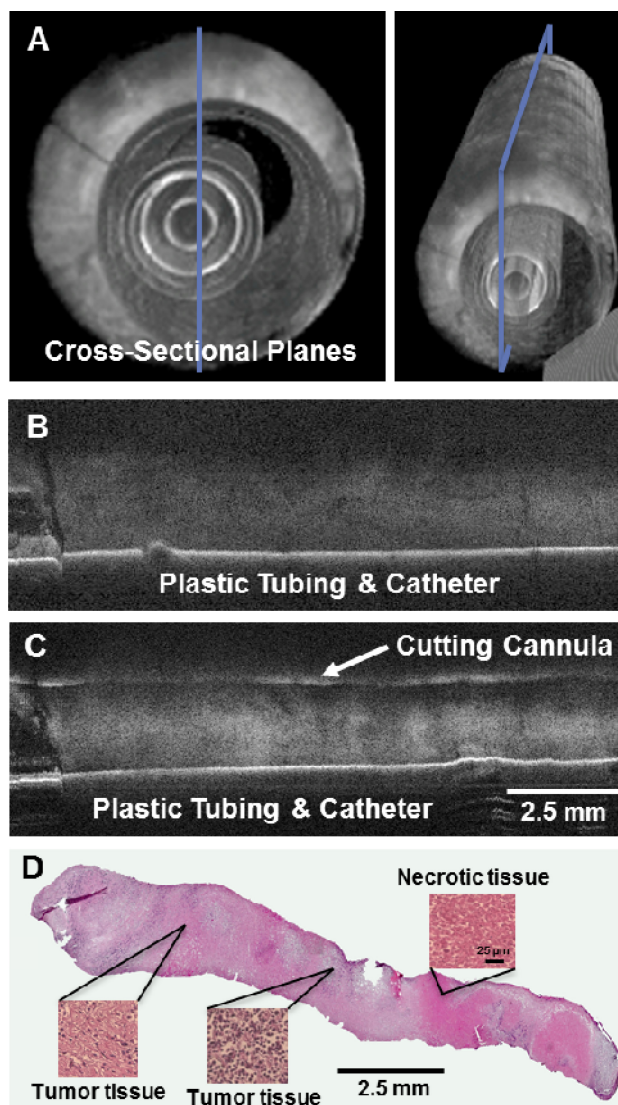
Fig. 6. Visualization of longitudinal (long-axis) cross-sectional planes of tissue data prior to and after tissue biopsy. (A) Three-dimensional renderings of the acquired OCT data set, illustrating orientation of cross-sectional planes relative to catheter and needle. (B) Cross-sectional plane extracted before physical biopsy. (C) Cross-sectional plane of tissue specimen immediately after physical biopsy. (D) Corresponding histological section of physical biopsy specimen. Insets show magnified histology regions indicating areas of tumor and necrotic tissue. Orientation of histological specimen is approximately that shown in (B) and (C).

4. Discussion

There exists an urgent need for more precise positioning and real-time image guidance of needle biopsies. Our increasing ability to image and detect smaller abnormal masses and lesions using clinical modalities such as MRI, x-ray CT, PET/SPECT, and ultrasound imaging mandates that we also advance the technology to physically biopsy these smaller suspicious tissues. The result will be fewer non-diagnostic specimens and fewer subsequent surgical procedures that would be required to access, remove, and histologically diagnose the suspicious lesions and masses found radiologically.

As previously stated, standard clinical imaging modalities are currently often used to coarsely guide the placement of needle biopsies, such as ultrasound, stereotactic x-ray imaging, or MRI guided breast needle biopsies, x-ray CT-guided needle biopsies for lung nodules and masses, or ultrasound-guided needle biopsies for thyroid nodules. However, most all of these are limited in their imaging resolution (millimeters), have large instrument footprints (MRI, CT), require extended set-up preparation and use time (30-60 minutes), and cannot provide immediate feedback on the quality of the tissue specimen prior to sending it to pathology for histological processing and diagnostic assessment, which often occurs 12-24 hours later. The compact 3-D OCT-guided core-needle biopsy system and methodology demonstrated here offers the potential to alleviate many of these practical limitations by providing fast, real-time optical image guidance of the actual needle tip and biopsy channel with micron-scale resolution, as well as the ability to image the tissue specimen immediately before and after the biopsy specimen has been collected, thereby providing a useful 3-D data set for evaluation, before the biopsy procedure ends, and before the specimens are sent off to the pathology department for standard histopathological processing and evaluation.

There have been numerous prior studies demonstrating the design and use of an OCT imaging needle [15,18–25]. In all of these prior studies, however, no design facilitated the real-time imaging of the tissue immediately before and after physical biopsy. Rather, their practical use would require the removal of the OCT needle and cessation of imaging, followed by the placement of a second hollow needle used for acquiring the physical biopsy. In addition, no prior needle design would enable direct 3-D imaging of the biopsied specimen, without having to physically remove the specimen and mount it in an external OCT microscope-stage configuration. We believe the advantages of this core-needle design overcome many of these prior practical limitations.

There are several limitations, however, that remain in this core-needle biopsy system that will need to be addressed for future clinical implementation. First, because of the wealth of 3-D OCT data that is possible with this design, fast computational processing, sectioning, and visualization will be needed to facilitate the comprehensive point-of-care evaluation of the image data during the procedure. Fortunately, the rapid advances being made in the implementation of graphical processing units (GPUs) for OCT and other medical imaging modalities will make this functionality feasible [26,27]. Second, for this initial demonstration, the inner metal/plastic tube to protect the OCT catheter was inserted into and positioned adjacent to the inner wall of the collection tube within the commercial hand-piece. This tube occupied 25% of the inner cross-sectional area of the needle, thereby reducing the cross-sectional area and volume of the biopsied tissue specimens. We do not believe, however, that this will significantly impact the quality of the tissue biopsy procedure, particularly since the added imaging capabilities are likely to improve tissue identification and biopsy, resulting in less tissue needed for biopsy. The additional metal/plastic tube, at times, restricted the vacuum-assisted transport of tissue specimens from the biopsy channel back to the tissue trap at the proximal end of the hand-piece. Future designs of this collection tube can be extruded to integrate the metal/plastic tube for the OCT catheter and minimize the crevasses where biopsied tissue specimens may get trapped and retained. Third, this prototype design utilized a relatively large gauge (9 Gauge) commercial biopsy needle. Future designs can reduce the diameter of the core-needle while still retaining the functional use of the OCT catheter. Future studies will demonstrate the use of this 3-D OCT-guided core-needle biopsy system *in vivo* in a large animal tumor model (porcine or canine) where the physical sizes of the body habitus and tumor tissue better approximate those found in humans.

In conclusion, we have demonstrated a novel 3-D OCT vacuum-assisted core-needle biopsy system that enables for the first time the ability to image small (sub-millimeter) target tissue immediately before and after physical biopsy. In addition, optical windows in the modified core-needle hand-piece enable real-time OCT guidance of the needle tip during insertion and while positioning the needle prior to tissue biopsy. With advantages over many

of the current modalities used for image guidance during needle biopsies, this system and methodology has the potential to improve our ability to biopsy the increasingly smaller lesions and masses now being identified by many clinical imaging systems.

Acknowledgments